

Voronoi diagrams, quasi-triangulations, and beta-complexes for disks in R^2 : the theory and implementation in BetaConcept

Jae-Kwan Kim¹, Youngsong Cho¹, Donguk Kim² and Deok-Soo Kim^{3,*}

¹ *Voronoi Diagram Research Center, Hanyang University, Seoul, South Korea*

² *Department of Industrial, Information, and Management Engineering, Gangneung-Wonju National University, Gangneung, Gangwon-do, South Korea*

³ *Department of Mechanical Engineering, Hanyang University, Seoul, South Korea*

(Manuscript Received September 17, 2013; Revised October 28, 2013; Accepted November 1, 2013)

Abstract

Voronoi diagrams are powerful for solving spatial problems among particles and have been used in many disciplines of science and engineering. In particular, the Voronoi diagram of three-dimensional spheres, also called the additively-weighted Voronoi diagram, has proven its powerful capabilities for solving the spatial reasoning problems for the arrangement of atoms in both molecular biology and material sciences. In order to solve application problems, the dual structure, called the quasi-triangulation, and its derivative structure, called the beta-complex, are frequently used with the Voronoi diagram itself. However, the Voronoi diagram, the quasi-triangulation, and the beta-complexes are sometimes regarded as somewhat difficult for ordinary users to understand. This paper presents the two-dimensional counterparts of their definitions and introduce the BetaConcept program which implements the theory so that users can easily learn the powerful concept and capabilities of these constructs in a plane. The BetaConcept program was implemented in the standard C++ language with MFC and OpenGL and freely available at Voronoi Diagram Research Center (<http://voronoi.hanyang.ac.kr>).

Keywords: Voronoi diagram of disks; Additively-weighted Voronoi diagram; Quasi-triangulations; Beta-complexes; Beta-shapes; Spherical atoms; GUI program

1. Introduction

Voronoi diagrams are powerful for solving spatial problems among particles in various disciplines [1]. The Voronoi diagram of three-dimensional spherical atoms, also called the additively-weighted Voronoi diagram, has shown its powerful capability to analyze molecular structures in both biology and material sciences in recent studies. However, we have learned that some users may regard the Voronoi diagram of atoms, its dual structure called the quasi-triangulation, and the beta-complexes somewhat difficult to understand. In this paper, we introduce the two-dimensional counterparts of their definitions and present the BetaConcept program, a GUI-based program for the Voronoi diagram, the quasi-triangulation, and the beta-complex in R^2 , with the following objectives:

- 1) To help users easily understand the concept of the Voronoi diagram, the quasi-triangulation, and the be-

ta-complex in R^2 ,

- 2) to help users identify applications of these constructs and test in the BetaConcept program (There are many important applications such as robot path planning, automatic car navigation, etc. in R^2), and
- 3) to help users extend their understanding to R^3 and motivate to use the BetaMol program [2], a molecular modeling, analysis, and visualization program for three-dimensional molecules.
- 4) In addition, this paper introduces two formal definitions: The *dual mapping* between the Voronoi diagram and the quasi-triangulation in R^2 and a new concept of the *quasi-simplicial complex* which we believe will play an important role in the theory in future.

We recommend readers to download and test the BetaConcept program freely available from the Voronoi Diagram Research Center (VDRC)(<http://voronoi.hanyang.ac.kr>). All figures in this paper were produced by the BetaConcept program. This paper is organized as follows: Section 2, 3, 4 present the theories of the Voronoi diagram of disks, the quasi-triangulation, and the beta-complex, respectively; Section 5 presents the BetaConcept program; Section 6 concludes the

*Corresponding author. Tel.: +82 2-220-0472, Fax.: +82 2-292-0472

E-mail address: dskim@hanyang.ac.kr

© 2014 Society of CAD/CAM Engineers & Techno-Press

paper.

2. Voronoi diagram of disks

Let $P = \{p_1, p_2, \dots, p_n\}$ be a set of points in \mathbb{R}^2 . The ordinary Voronoi diagram \mathcal{VD} of P is the tessellation of the space where the Voronoi cell $\mathcal{VC}(p_i)$ is a set of locations closer to p_i than to p_j , $i \neq j$. Let $A = \{a_1, a_2, \dots, a_n\}$ be a set of disks $a_i = (p_i, r_i)$ with the center p_i and the radius r_i in \mathbb{R}^2 . The Voronoi cell (V-cell) $\mathcal{VC}(a_i)$ for a_i is defined as $\mathcal{VC}(a_i) = \{x \in \mathbb{R}^2 \mid \text{dist}(x, p_i) - r_i \leq \text{dist}(x, p_j) - r_j \text{ for } i \neq j\}$ where $\text{dist}(x, y)$ denotes the Euclidean distance between $x, y \in \mathbb{R}^2$. Then, the Voronoi diagram \mathcal{VD} of A , also called the additively-weighted Voronoi diagram, is defined as $\mathcal{VD} = \{\mathcal{VC}(a_1), \mathcal{VC}(a_2), \dots, \mathcal{VC}(a_n)\}$. The connectivity among the vertices, edges, and cells in \mathcal{VD} can be stored in a data structure such as the winged-edge or half-edge data structure because of its planarity property. The BetaConcept program adapted the winged-edge data structure. Its counterpart of the Voronoi diagram of spheres in \mathbb{R}^3 can be stored in the radial-edge data structure [3]. \mathcal{VD} is represented by a triplet (V^\vee, E^\vee, C^\vee) where V^\vee, E^\vee , and C^\vee are the sets of Voronoi vertices (V-vertices), Voronoi edges (V-edges), and Voronoi cells (V-cells), respectively. For the details of the properties and algorithms of \mathcal{VD} in the three-dimensional space, see [4, 5]. For the topology data structure, see [6].

There have been several studies on the Voronoi diagram of disks and related problems. Lee and Drysdale considered the problem of the Voronoi diagram for a set of non-intersecting disks and proposed an algorithm running in $O(n \log^2 n)$ [7]. Sharir reported an algorithm computing the Voronoi diagram of a disk set in $O(n \log^2 n)$, where the disks may intersect [8]. Yap reported a $O(n \log n)$ algorithm for computing the Voronoi diagram of closed polygons consisting of line segments and arc [9]. Gavrilova and Rokne reported an algorithm which maintains a valid data structure when disks are dynamically moving [10]. Sugihara reported an approximation algorithm for a disk set using the powerful capability of the topology-oriented robust computation of the ordinary Voronoi diagram of points [11]. Kim et al. developed an edge-flipping algorithm which computed the Voronoi diagram of disks by flipping edges of the ordinary Voronoi diagram of points in $O(n^2)$ time in the worst case [12, 13]. We prefer the name “the Voronoi diagram of disks” to “the additively-weighted Voronoi diagram” for the sake of user intuition and in favor of applications. The BetaConcept program is based on the Kim and colleagues edge-flipping algorithm for the Voronoi diagram of disks computed from the ordinary Voronoi diagram of points, it uses Sugihara’s code of the topology-oriented robust algorithm.

Figure 1(a) is the ordinary Voronoi diagram \mathcal{VD} of a set P of points and Figure 1(b) is the Voronoi diagram \mathcal{VD} of a set A of disks where each point in P has an associated circular atom with an assigned radius. Note that the tiny atom between the two largest atoms has a V-cell bounded by only two V-edges. We call that the tiny atom is associated with a

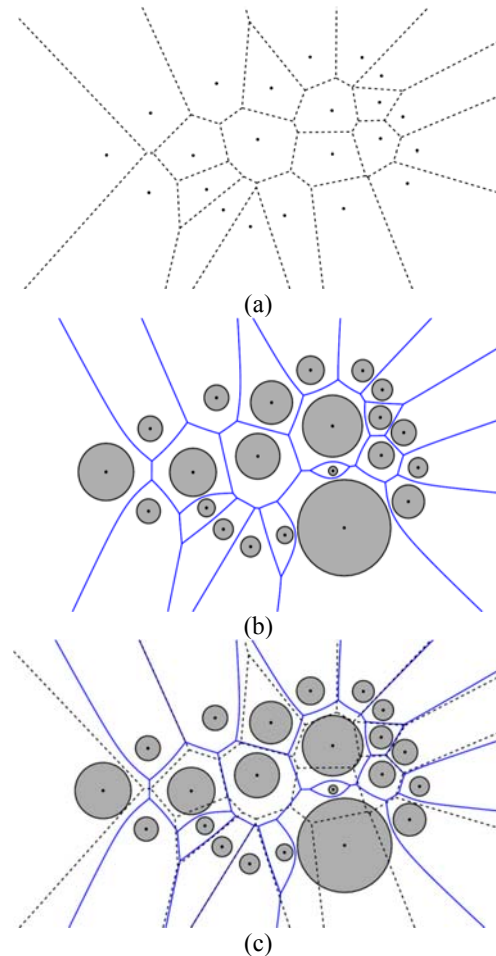


Figure 1. The Voronoi diagram of points and disks: (a) the Voronoi diagram \mathcal{VD} of points, (b) the Voronoi diagram \mathcal{VD} of disks, (c) the superposition.

2-edge bounded V-cell. Figure 1(c) shows the superposition of \mathcal{VD} and \mathcal{VD} . Check the similarity and dissimilarity between \mathcal{VD} and \mathcal{VD} : An edge of \mathcal{VD} is flipped in \mathcal{VD} .

3. Quasi-triangulation

Voronoi diagrams are frequently stored in their dual structures for both the convenience and efficiency from both storage and query process point of view. The dual of the ordinary Voronoi diagram \mathcal{VD} of points is the Delaunay triangulation \mathcal{DT} which is a simplicial complex. The dual structure of the Voronoi diagram \mathcal{VD} of disks is called the quasi-triangulation \mathcal{QT} which may be a non-simplicial complex in general [14, 15].

Definition 1. Let \mathcal{D} be a dual operator which transforms \mathcal{VD} to \mathcal{QT} in \mathbb{R}^2 as follows:

- $\mathcal{D} : c^\vee \Rightarrow v^\mathcal{Q}$ is a mapping from a V-cell $c^\vee \in C^\vee$ to a qt-vertex $v^\mathcal{Q} \in V^\mathcal{Q}$. The coordinate of the qt-vertex $v^\mathcal{Q}$ is the center p of the disk a corresponding to the V-cell c^\vee .

- $\mathcal{D} : e^V \Rightarrow e^Q$ is a mapping from a V-edge $e^V \in E^V$ to a qt-edge $e^Q \in E^Q$. The qt-edge e^Q is a line segment bounded by v_i^Q and v_j^Q , for distinct i and j , where the disks a_i and a_j define the V-edge e^V .
- $\mathcal{D} : v^V \Rightarrow f^Q$ is a mapping from a V-vertex $v^V \in V^V$ to a qt-face $f^Q \in F^Q$. The qt-face f^Q is a topological triangle bounded by three vertices v_i^Q , v_j^Q , and v_k^Q , for distinct i, j , and k , which correspond to the three disks defining the V-vertex v^V . Each pair of qt-vertices defines a qt-edge e^Q of f^Q . The orientation of f^Q is critical and should be consistent with the angular ordering of the V-edges incident to v^V .

Figure 2 illustrates an example of the dual mapping \mathcal{D} . The qt-vertices v_1^Q, v_2^Q and v_3^Q in Figure 2(b) are transformed from the V-cells c_1^V, c_2^V , and c_3^V in Figure 2(a), respectively. Hence, the coordinates of the qt-vertices are from the coordinates of the centers of the disks corresponding to the V-cells. The qt-edges e_1^Q, e_2^Q and e_3^Q are from the V-edges e_1^V, e_2^V and e_3^V , respectively. The qt-face f_1^Q is from the V-vertex c_1^V . In the mapping \mathcal{D} , the orientations of the qt-edges and the qt-face are carefully maintained. The reverse mapping, \mathcal{D}^{-1} , from QT to VD can also be similarly defined. The dual map \mathcal{D} between VD and QT is, in a way, similar to the dual map between VD and DT . Briefly speaking, in the plane, \mathcal{D} maps a V-cell to a qt-vertex, a V-edge to a qt-edge,

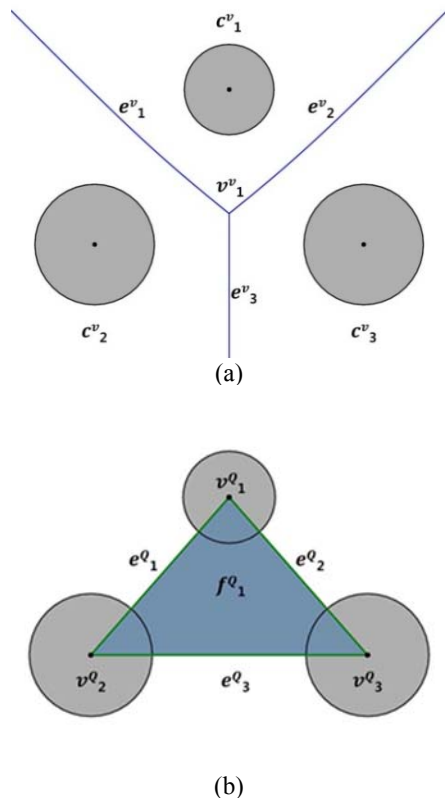


Figure 2. The dual mapping \mathcal{D} as follows: (a) Voronoi diagram of three circles, (b) transformed quasi-triangulation.

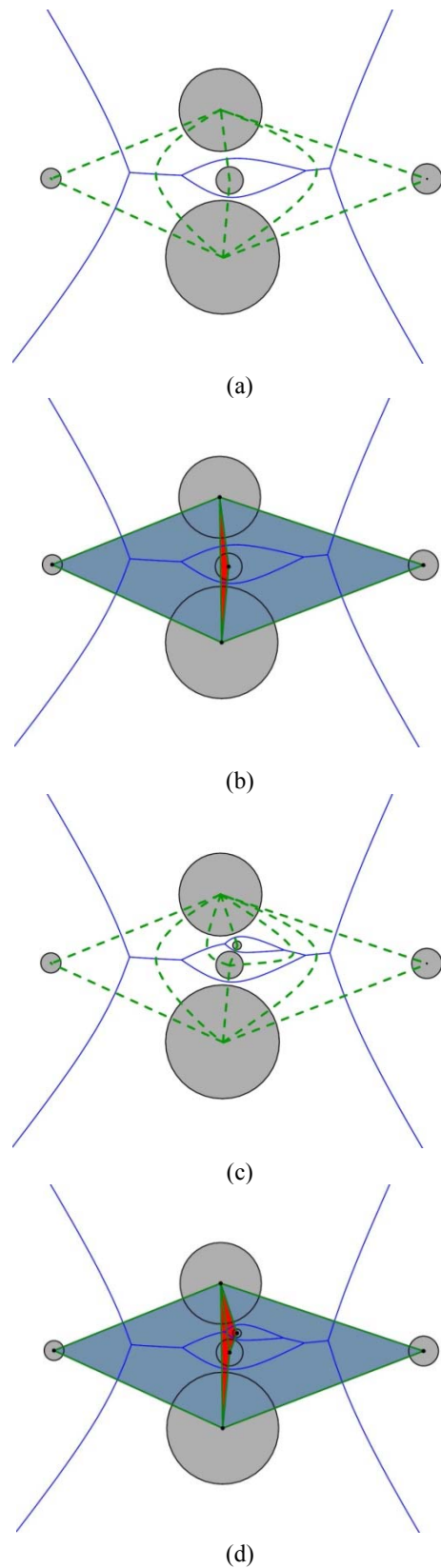


Figure 3. Anomalies in QT : (a) anomaly in schematic QT with VD , (b) anomaly in real QT , (c) and (d) anomalies occurring in a nested form.

and a V-vertex to a qt-cell. Then, the quasi-triangulation can be represented by a triplet $QT = (V^Q, E^Q, F^Q)$ where V^Q , E^Q , and F^Q are the sets of vertex simplexes (qt-vertices), edge simplexes (qt-edges), and triangular cell simplexes (qt-cells), respectively. Hence, QT correctly defines the proximity among disks and is equivalent to VD from the topological point of view. VD can be transformed to QT in $O(m)$ time in the worst case where m represents the number of simplexes in QT . For the detailed definition and properties of the quasi-triangulation in a more general setting of three-dimensional spaces, see [14, 15].

It is well-known that the Delaunay and the regular triangulations are a simplicial complex which is powerful to answer to various geometric and topological queries. However, it was earlier observed that the quasi-triangulation in R^3 possesses properties which violate the condition for a simplicial complex [14, 15]. Until now, a complex is only considered a general class of non-simplicial complex if it does not satisfy the condition of a simplicial complex. In this paper, we propose a distinct class of non-simplicial complex which is defined as follows:

Definition 2. C is a quasi-simplicial complex if it satisfies the following two conditions:

- Any face of an element in C is also in C , and
- two elements in C intersect at one or more lower-dimensional face, if it does.

Be aware that this definition is a slight generalization of that of simplicial complex. Two k -simplexes in C can share up to $k+1$ common $(k-1)$ -simplexes in R^d where $k \leq d$.

It turns out that the quasi-triangulation is a quasi-simplicial complex. Figure 3 illustrates an example. Figure 3(a) shows five disks and the Voronoi diagram VD (shown in solid curves). The green broken curves (with two bent curves) denote the schematic diagram of the dual mapping of VD and thus they altogether present the topology of the quasi-triangulation QT . Note that each green broken curve corresponds to a V-edge and there are two triangles defined by two big disks and a small disk in the middle. Figure 3(b)

shows the real QT obtained by straightening the bent curves. Note that the two schematic triangles bounded by the green broken edges do not overlap and thus they are topologically distinct. However, the two green broken triangles map to two identical-looking skinny triangles (bounded by green solid line segments) in QT in Figure 3(b). The red-colored triangle denotes this fact and thus implies that there are two superposed ones from geometric point of view. This phenomenon is called an *anomaly*. Figures 3(c) and 3(d) show that such an anomaly can occur in a nested form.

Data structures to store QT and VD are of importance. While DT can be stored in the simplicial complex data structure (SCDS), QT needs a specialized variation known as the inter-world data structure (IWDS). See Kim et al. [14] for details of IWDS in R^3 . It is, however, interesting to observe that, in R^2 , the IWDS reduces to SCDS. From topological point of view, the difference between QT and DT in R^2 is the following: In DT, two triangular faces can share at most one edge, but in QT , two triangular faces can share one or two edges. This property of QT can be incorporated into SCDS in that two incident face pointers have identical values.

Figures 4(a) and 4(b) show the schemas of the (standard full) winged-edge data structure for the Voronoi diagrams and the inter-world data structure for the quasi-triangulation in the BetaConcept program, respectively. The integer next to an arrow denotes the number of pointers. The data structure in Figure 4(b) can be further compactly made as Figure 4(c) if the queries are only for the topology traversal among simplexes. BetaConcept explicitly represents edge-simplexes. Note that the schema in Figure 4(c) is also a popular way of storing the topology of the Delaunay triangulation.

Figure 5 shows the quasi-triangulation corresponding to the Voronoi diagram in Figure 1(b). Note that there is a skinny red triangle between the two largest disks. This seemingly one triangle is in fact the superposition of two triangles: one dual-mapped from each of the two Voronoi vertices existing on the Voronoi edge between the two largest disks in the Voronoi diagram. In such a case, one triangle is clockwise

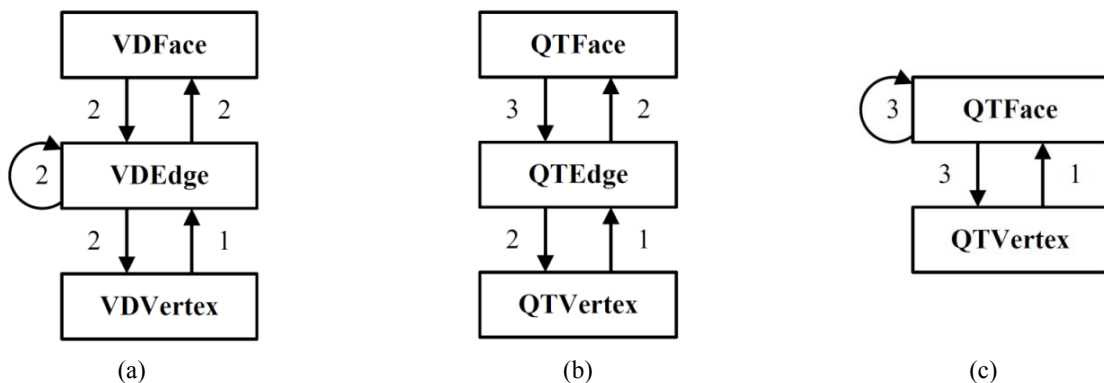


Figure 4. Data structure schemas: (a) the winged-edge data structure (WEDS) used for VD , (b) the inter-world data structure (IWDS) used for QT , (c) the compressed version of IWDS.

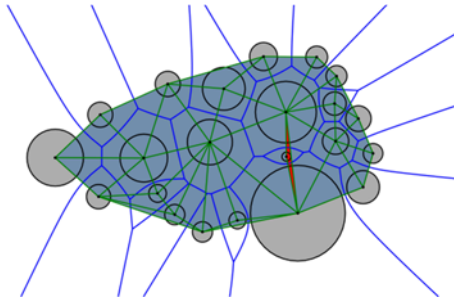


Figure 5. Quasi-triangulation of the Voronoi diagram in Figure 1(b).

oriented (with a negative signed area) and the other is counterclockwise oriented (with a positive signed area). The red colored triangle corresponds to the one with the negative signed area. This intriguing case is called the anomaly case and is the only one anomaly case in the plane. In the three-dimensional case, there are other anomaly cases and for the details, see [16].

4. Beta-complex

Suppose that we select a qt-edge e (connecting a pair of atom centers) from QT and consider a circular probe with the radius β . Suppose that we move the probe around the two atoms and test if the probe can move freely between the two atoms without simultaneously intersecting both atoms. If the probe can pass, we remove e from QT . Otherwise, we leave it in QT . We repeat this operation for all the qt-edges in QT . Now, we select a qt-cell f (connecting a triplet of atom centers) from QT . We check if it is possible to place the probe among the three atoms so that it can be free of intersection with all three atoms at the same time. If it can be placed, we remove the qt-cell from QT . Otherwise, we leave the qt-cell in QT . We also repeat this operation for all qt-cells in QT . Then, we are left with a subset of QT which corresponds to an object called the *beta-complex* BC corresponding to the probe. Hence, the beta-complex is a subset of the quasi-triangulation where its boundary is defined by the size of the probe (i.e., the probe radius). The region of the space bounded by the boundary of the beta-complex is called the *beta-shape* BS . For details in R^3 , see [17].

The description above tells us that the extraction of the beta-complex from the quasi-triangulation is in fact a search problem for appropriate simplexes. This search can be done efficiently if the simplexes are classified according to their states as follows and sorted using a parameter indicating the range of probe radius. Suppose that σ is a qt-edge. Then, σ is called *singular* if the probe can touch σ at exactly two locations; *regular* if the probe can touch σ at only a single location; *interior* if the probe cannot touch σ ; Otherwise (i.e., the probe can freely pass through σ), σ is *exterior*. Suppose that σ is a qt-vertex. Then, σ is *singular* if the locus of the probe centers touching σ is a complete circle and is *regular* if the

Table 1. Rules to compute the β -intervals of simplexes in the 2D quasi-triangulation.

Simplexes and Their Local Configurations		Rule	Bounding State		
			Singular	Regular	Interior
Triangular Face		1			$[\rho_{\bar{A}}, \infty)$
Edge	$\notin \partial SH(A)$, unattached	2	$[\rho_{\bar{A}}, \mu_{\bar{A}})$	$[\mu_{\bar{A}}, \bar{\mu}_{\bar{A}})$	$[\bar{\mu}_{\bar{A}}, \infty)$
	$\notin \partial SH(A)$, attached	3		$[\mu_{\bar{A}}, \bar{\mu}_{\bar{A}})$	$[\bar{\mu}_{\bar{A}}, \infty)$
	$\in \partial SH(A)$, unattached	4	$[\rho_{\bar{A}}, \mu_{\bar{A}})$	$[\mu_{\bar{A}}, \infty)$	
	$\in \partial SH(A)$, attached	5		$[\mu_{\bar{A}}, \infty)$	
Vertex	$\notin \partial SH(A)$	6	$[-\infty, \mu_{\bar{A}})$	$[\mu_{\bar{A}}, \bar{\mu}_{\bar{A}})$	$[\bar{\mu}_{\bar{A}}, \infty)$
	$\in \partial SH(A)$	7	$[-\infty, \mu_{\bar{A}})$	$[\mu_{\bar{A}}, \infty)$	

locus is one or more arc. In all cases, σ is *interior* if the probe cannot touch σ at any location. A qt-vertex is never exterior. Suppose that σ is a qt-face. Then, σ is *interior* if the probe cannot be placed in the middle of three disks unless it intersects one or more disk. Otherwise, σ is *exterior*.

Table 1 summaries the detailed search rule used to extract the beta-complex from the quasi-triangulation based on the states of simplexes. The inter-world data structure schema of Figure 4(b) is adapted in the BetaConcept program because the edge-simplexes should be explicitly represented to store the intervals, called the beta-interval, for each edge. For the details of the rule, see [17]. For the inter-world data structure in R^3 , see [14]. The simplex search for beta-complexes can be done in $O(\log m)$ time in the worst case where m is the number of simplexes in the quasi-triangulation [17]. The computational issue for the simplex search was discussed for general queries in [18].

Figure 6(a) shows the input disk generators and the quasi-triangulation. Figures 6(b) through 6(f) are the beta-complexes for various probes of increasing size from a small value to infinity. Figure 6(c) shows the anomaly triangle in the quasi-triangulation does not appear whereas Figure 6(d) shows that the anomaly triangle (the skinny red face) appears in the beta-complex when the probe size slightly increases. Recall that the red triangular face is in fact two triangles. Figure 6(f) is the beta-complex corresponding to the probe size of infinity and is identical to the quasi-triangulation.

Suppose that we collect the vertices and edges on the boundary of the beta-complex and consider that the interior of the boundary is filled with a material. Then, the filled object is thus the beta-shape and has the following properties: i) It may consist of polygons with their interior filled; ii) It may consist of edges connecting polygons; iii) It may have dangling edges; iv) Two polygons may touch each other at a vertex; or v) It may have disconnected components (such as vertices, edges, and/or polygons). Hence, a beta-shape can be non-manifold. In the three-dimensional case, see [17].

5. The BetaConcept program

The BetaConcept program was developed with a standard

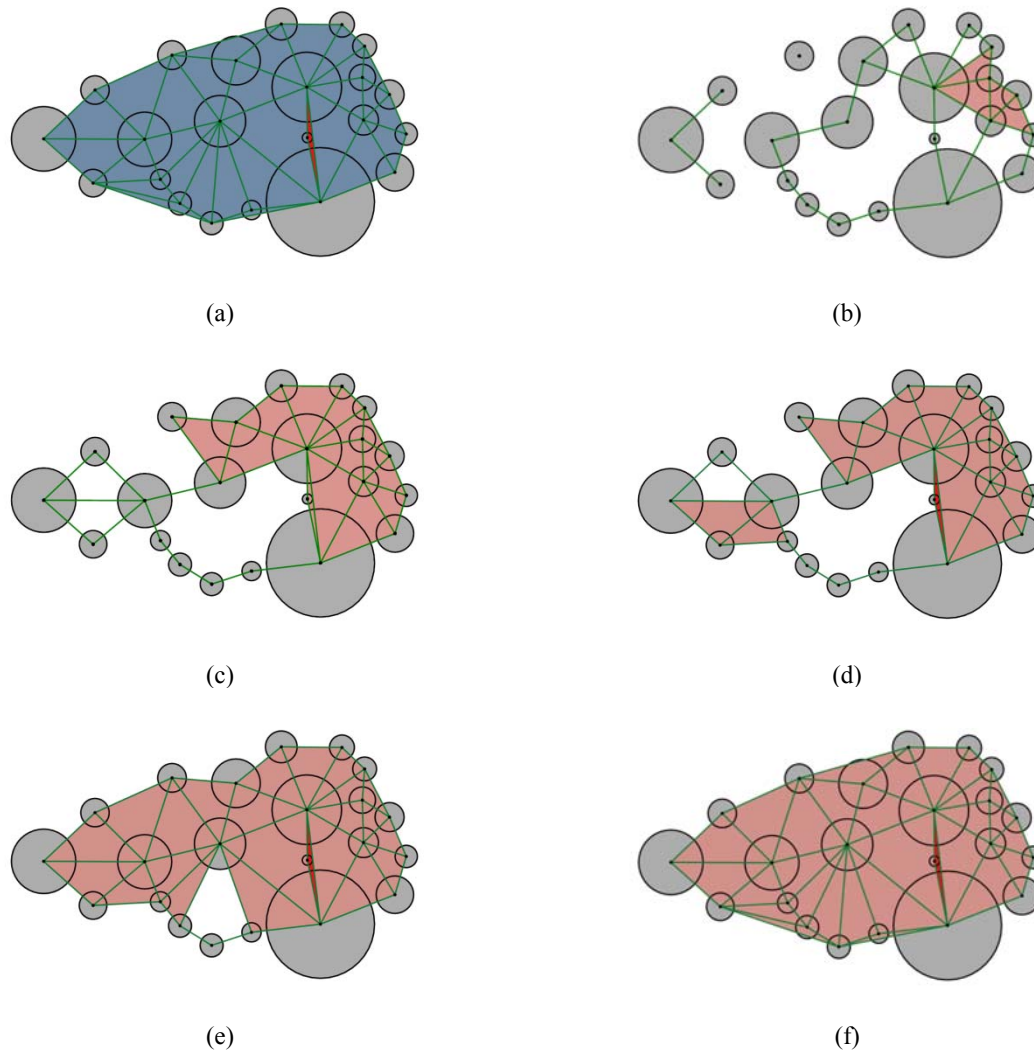


Figure 6. A set of disk generators, the quasi-triangulation, and the beta-complexes corresponding to different probe values of the radius β : (a) the input disks with QT , (b) BC for a tiny $\beta_1 > 0$, (c) BC for $\beta_2 > \beta_1$ (no anomaly), (d) BC for $\beta_3 > \beta_2$ (an anomaly), (e) BC for $\beta_4 > \beta_3$, and (f) BC for $\beta_5 = \infty$ (BC is identical to QT).

C++, the MFC for user interface, and the OpenGL for its graphics and consists of six groups of functions:

- Creation, selection, modification, and deletion of disk generators
- The computation of VD/VDs , the transformation to DT/QT , the extraction of BC , and the analysis of their statistics
- Offsetting and blending
- File i/o
- Attribute editing
- Replay of the system status

The graphical user interface of the BetaConcept program, shown in Figure 7, consists of three sections: the graphical display, the statistics display (bottom-left), and the menu for user's control of the program (right). An online manual can be invoked by clicking the button at the top-right on the

screen.

5.1 Creation, selection, deletion, and transformation of disk generators

Users can create disk generators in two ways: i) One-at-a-time creation by dragging the left-button-pressed mouse while the "ctrl" key is also pressed and ii) a grid-template creation by clicking the button on the menu panel. Users can determine the size of a grid by providing parameters. Figure 8(a) shows two clusters of disk generators created: One by one-at-a-time approach and the other by the grid-template creation for the matrix of 3×5 .

There are two ways to select disks: i) Clicking the left button on the top of the disk to choose and ii) using a rubber-banding by dragging the left-button-pressed mouse while the "shift" key is pressed. The rubber-banding method can select

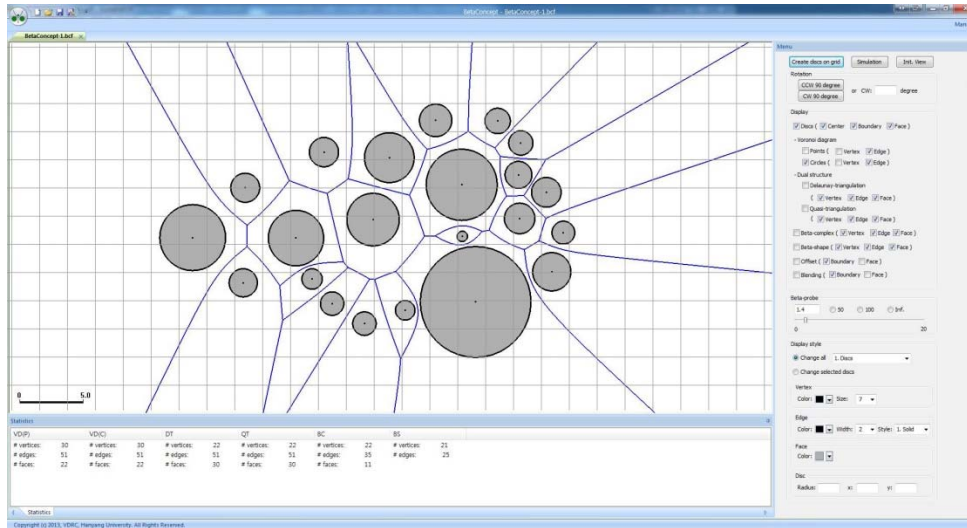


Figure 7. The BetaConcept program graphical user interface.

a group of disks in a rectangular range. Selected disks can be either deleted by simply pressing the “delete” key or their attributes can be modified.

All created generators can be translated with mouse and rotated with the menu and the transformed generators can return to the initial view. Zoom-in and zoom-out are also provided.

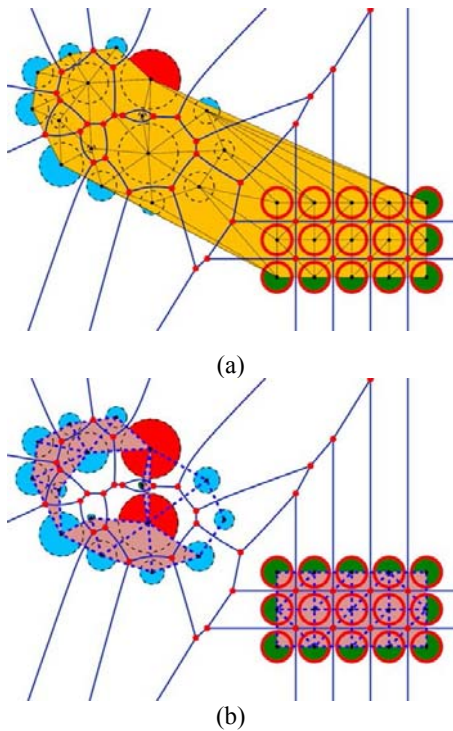


Figure 8. Diverse ways to assign attributes to the entities in the BetaConcept program: (a) generators, the Voronoi diagram, and the quasi-triangulation, (b) generators, the Voronoi diagram, and the beta-complex.

5.2 Attribute editing

Users can edit the attributes of selected entities. In the case of a disk, the user can modify both the geometry (i.e., coordinates and radius) and the presentation style such as the color, thickness, style of the disk. A disk can also be filled with different colors. Other entities such as the Voronoi diagrams, the quasi-triangulation, the beta-complex, the beta-shape, etc. can also be modified in a similar manner. In Figure 8(a), different colors are used to fill the disk generators and the quasi-triangulation is also colored differently. Figure 8(b) shows the beta-complex with attributes edited.

5.3 Computation of VD , QT , and BC

The BetaConcept program computes the VD when more than three disks are created and transforms it to QT . Users can extract the BC from the QT by setting the probe radius, i.e., a β -value. The β -value can be set by either adjusting a slide bar or typing the value on the menu. The VD , QT , and BC can be displayed independent to each other by checking/unchecking the box on the menu. Users can change the visibility of the each simplexes (i.e., visibility of vertices, edges, or faces) and change the style of each simplex. The statistics of the VD , the QT , and the BC are displayed in the statistics panel. If the status of any of them changes, the statistics will be change automatically.

5.4 File i/o

The BetaConcept program has three modes of file i/o. The disk generators can be stored in an ASCII file and can be later loaded again. The current visualization in the graphics panel can also be stored in a PDF file so that it can be used in documents. All graphical figures in this paper were produced using this function. The user can load a bitmap image file as the background as shown in Figure 9.

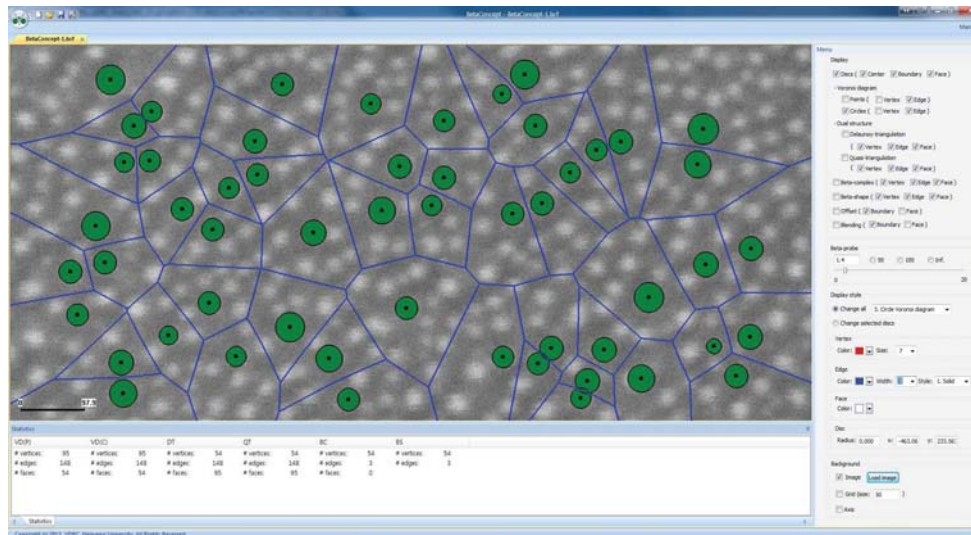


Figure 9. The BetaConcept program with a background bitmap image.

5.5 Simulation (replay)

The BetaConcept program maintains the session status by the order of either the creation of the disks currently displayed or by users' choice. Thus, by triggering the creation sequence of the input disks in this order, users can catch the status change by incrementing disks one by one. We call this process a simulation. In other words, the user can simulate the changes of \mathcal{VD} , \mathcal{QT} , and \mathcal{BC} by activating the simulation function by clicking the "simulation" button on the menu which has two options: automatic and manual. If the user chooses the automatic option and sets the time interval in the unit of second, the program shows the status change by incrementing disks one by one with the defined time interval. If the user chooses the manual, users can increment disk one by one by clicking the next button on the control panel.

5.6 Offsetting and blending

The BetaConcept program can compute a trimmed offset with the offset amount $\delta > 0$. The computation of blending is also similar to the offset computation. The program first computes the beta-shape \mathcal{BS} for $\beta = \delta$ and then extracts the boundary $\partial\mathcal{BS}$ to store in a graph data structure $G = (V^G, E^G)$. A singular edge $e^G \in E^G$ means that its two incident qt-cells are exterior and a regular edge means that one of its two incident qt-cells is exterior and the other is interior.

G is in general a forest. Suppose that $G = \{\xi_1, \xi_2, \dots, \xi_m\}$ where $\xi \in G$ is a component. For each component ξ of G , the program does the following. If all edges in ξ is regular, its graph structure is directly used for connecting offset arcs. Otherwise, it duplicates each singular edge and creates a loop structure with proper orientation. Note that the orientation of each edge provides the information how to choose the intersection point between two intersection points between two atom boundaries. Given a beta-shape \mathcal{BS} , the offset-

computing algorithm is easy and obvious and its computational complexity is $O(m)$ in the worst case where m represents the number of edges on ξ . Note that $m = O(n)$ in the worst case in \mathbb{R}^2 . The idea inherits the earlier one in [19].

Figure 10 shows the offset and blends with the Voronoi diagram \mathcal{VD} and the beta-shape \mathcal{BS} for four different probes. In each figure, the black disks are the input disks and the shaded disks are the offset disks. Note that the boundary of the offset is correctly computed and the intersection between consecutive arcs are precisely located on the Voronoi diagram \mathcal{VD} . The red chain is the boundary of the blended disks defined by the probe. Both the offsets and blends are computed using the beta-shape shown inside the shaded region.

6. Conclusions

In this paper, we presented the definition of the dual mapping between the Voronoi diagram and the quasi-triangulation in the plane. In particular, we introduced the notion of the quasi-simplicial complex for the first time and showed that the quasi-triangulation is a quasi-simplicial complex. We also introduced the BetaConcept program which is the implementation of the two-dimensional Voronoi diagrams, quasi-triangulations, and their beta-complexes. The BetaConcept program can help users to learn about the powerful concept and capabilities of the Voronoi diagram, the quasi-triangulation, and the beta-complex in the plane and hopefully extend the understanding to their three-dimensional counterparts. By using this program, users can also identify applications of these constructs in the plane. We welcome any suggestions and collaborations for these constructs, BetaConcept, and BetaMol.

Acknowledgments

This work was supported by the National Research Founda-

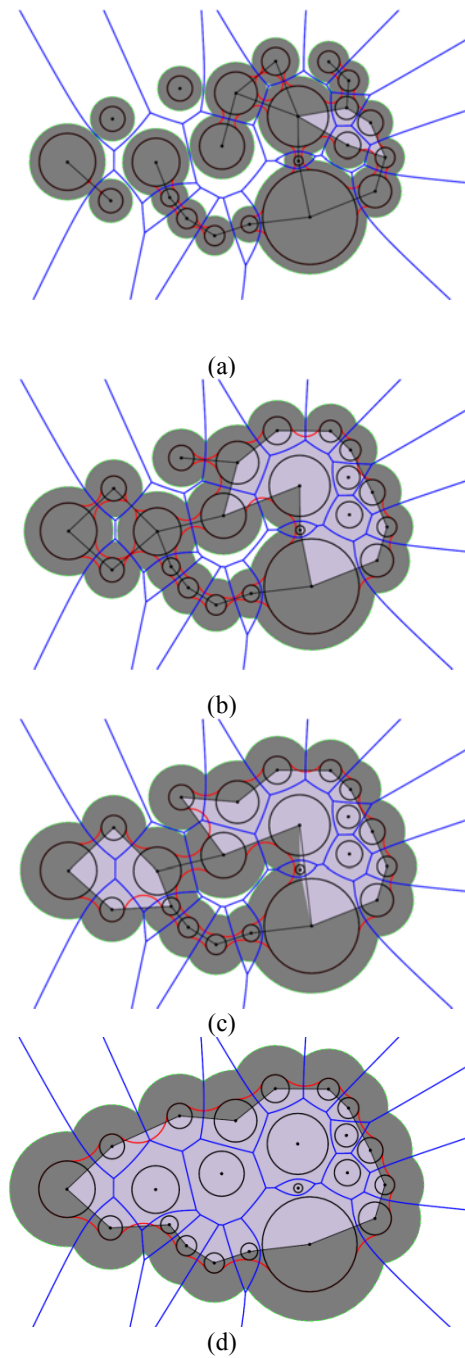


Figure 10. The offset and blends with VD and BC for given input disks: (a) for a tiny probe with $\beta_1 > 0$, (b) for a small probe ($\beta_2 > \beta_1$), (c) for a medium probe ($\beta_3 > \beta_2$), and (d) for a large probe ($\beta_4 > \beta_3$).

tion of Korea (NRF) grant funded by the Korea government (MSIP) (No. 2012R1A2A1A05026395).

References

[1] Okabe A, Boots B, Sugihara K, Chiu SN. Spatial tessellations:

- Concepts and applications of Voronoi diagrams. 2nd ed. Chichester: John Wiley & Sons; 2000. 696 p.
- [2] Cho Y, Kim JK, Ryu J, Won CI, Kim CM, Kim D, Kim DS. BetaMol: A molecular modeling, analysis and visualization software based on the beta-complex and the quasi-triangulation. *Journal of Advanced Mechanical Design, Systems, and Manufacturing*. 2012; 6(3): 389-403.
- [3] Cho Y, Kim D, Kim DS. Topology representation for the Voronoi diagram of 3D spheres. *International Journal of CAD/CAM*. 2005; 5(1): 59-68.
- [4] Kim DS, Cho Y, Kim D. Euclidean Voronoi diagram of 3D balls and its computation via tracing edges. *Computer-Aided Design*. 2005; 37(13): 1412-1424.
- [5] Kim D, Kim DS. Region-expansion for the Voronoi diagram of 3D spheres. *Computer-Aided Design*. 2006; 38(5): 417-430.
- [6] Lee K. Principles of CAD/CAM/CAE systems. Upper Saddle River (NJ): Prentice Hall; 1999. 640 p.
- [7] Lee D, Drysdale R. Generalization of Voronoi diagrams in the plane. *SIAM Journal on Computing*. 1981; 10(1): 73-87.
- [8] Sharir M. Intersection and closest-pair problems for a set of planar discs. *SIAM Journal on Computing*. 1985; 14(2): 448-468.
- [9] Yap CK. An $O(n \log n)$ algorithm for the Voronoi diagram of a set of simple curve segments. *Discrete & Computational Geometry*. 1987; 2: 365-393.
- [10] Gavrilova M, Rokne J. Swap conditions for dynamic vd for circles and line segments. *Computer Aided Geometric Design*. 1999; 16(2): 89-106.
- [11] Sugihara K. Approximation of generalized Voronoi diagrams by ordinary Voronoi diagrams. *Graphical Models and Image Processing*. 1993; 55(6): 522-531.
- [12] Kim DS, Kim D, Sugihara K. Voronoi diagram of a circle set from Voronoi diagram of a point set: I. topology. *Computer Aided Geometric Design*. 2001; 18: 541-562.
- [13] Kim DS, Kim D, Sugihara K. Voronoi diagram of a circle set from Voronoi diagram of a point set: II. geometry. *Computer Aided Geometric Design*. 2001; 18: 563-585.
- [14] Kim DS, Kim D, Cho Y, Sugihara K. Quasi-triangulation and interworld data structure in three dimensions. *Computer-Aided Design*. 2006; 38(7): 808-819.
- [15] Kim DS, Cho Y, Sugihara K. Quasi-worlds and quasi-operators on quasi-triangulations. *Computer-Aided Design*. 2010; 42(10): 874-888.
- [16] Kim DS, Cho Y, Ryu J, Kim JK, Kim D. Anomalies in quasi-triangulations and beta-complexes of spherical atoms in molecules. *Computer-Aided Design*. 2013; 45(1): 35-52.
- [17] Kim DS, Cho Y, Sugihara K, Ryu J, Kim D. Three-dimensional beta-shapes and beta-complexes via quasi-triangulation. *Computer-Aided Design*. 2010; 42(10): 911-929.
- [18] Kim DS, Kim JK, Cho Y, Kim CM. Querying simplexes in quasi-triangulation. *Computer-Aided Design*. 2012; 44(2): 85-98.
- [19] Kim DS. Polygon offsetting using a Voronoi diagram and two stacks. *Computer-Aided Design*. 1998; 30(14): 1069-1076.